kcal/mol below the syn alternative in water. The poorer hydration that accompanies rotation from the ground state to the anti transition state was found to result from diminished hydrogen bonding to the carbonyl oxygen that is not made up by introduction of limited hydrogen bonding at the pyramidalized nitrogen. The enhanced hydration of the syn transition state results in part from greater hydrogen bonding in the region of confluence of the figurative nitrogen and oxygen lone pairs, and from more constructive longer-range interactions with water molecules. The solvent effects in CCl_4 are much less with the anti and syn transition states destabilized by 0.38 and 0.05 kcal/mol relative to the ground state. Thus, with addition of the gas-phase free energy difference, the syn transition state is not competitive in CCl_4. The predicted, substantial increase in $\Delta G^{\ddagger}$ between dilute CCl_4 and aqueous solution, 1.7 kcal/mol, is consistent with experimental estimates; however, the present calculations find a 1-2-kcal/mol smaller difference between the gas phase and CCl_4 solution than has been reported experimentally. The potential functions developed here may also be useful in future calculations for the transmission coefficient and for modeling related isomerizations in real and artificial enzymes.

Acknowledgment. Gratitude is expressed to the National Science Foundation and National Institutes of Health for support of this research, and to Professor Donald G. Truhlar for helpful insights.

Molecular Recognition of Potassium Ion by the Naturally Occurring Antibiotic Ionophore Nonactin

Tami J. Marrone and Kenneth M. Merz, Jr.*

Contribution from the Department of Chemistry, The Pennsylvania State University, University Park, Pennsylvania 16802. *Received March 13, 1992*

Abstract: Potential of mean force (PMF), free energy perturbation (FEP), and molecular dynamics (MD) computer simulations have been used to investigate the molecular recognition of K^+ by the ionophore nonactin in methanol. First, parameter sets for K^+ and Na^+ in methanol were developed such that they were able to reasonably reproduce the free energy of solvation of these ions as well as coordination numbers. Next, we computed the free energy of binding difference for $K^+ \rightarrow Na^+$ in nonactin and obtained a value of 1.0 ± 0.8 kcal/mol which is in good agreement with the experimental value of 2.0 ± 0.7 kcal/mol. To obtain an estimate of the absolute free energy of binding, we used PMF calculations. This was done only for K^+, and we found that our calculated binding energy was in good agreement with the experimental one (−6.4 kcal/mol versus -5.5 ± 0.6 kcal/mol). Analysis of the structures obtained along the PMF pathway yielded interesting details about the complexation process in nonactin. A brief discussion of the function of nonactin is also presented.

Introduction

Understanding at the molecular level how one molecule recognizes another is of fundamental importance to chemistry and biochemistry.[1] Antibiotic ionophores, such as valinomycin and the macrotetralide nonactin, have been studied in detail in order to understand how these molecules selectively recognize ions.[2] These naturally occurring molecules selectively bind a specific metal ion, which can be considered as a charged spherical "substrate", and transport it across the cell membrane to release it on the other side.[2] Under certain circumstances, synthetic macrocycles are also capable of performing this function.[3] Generally, ionophores preferentially bind a specific metal ion, but the selectivity scale varies widely among the naturally occurring ionophores with valinomycin having one of the highest K^+/Na^+ selectivities and nonactin having a lower K^+/Na^+ selectivity.[2] For these molecules to accomplish their transport function they must have several characteristics. First they must be able to bind a metal ion selectively and tightly while at the same time be flexible enough to release the ion fairly rapidly. Furthermore, to be compatible with a biomembrane, the ionophore must have a hydrophobic exterior while having a hydrophilic interior capable of binding an ion. Nonactin meets these requirements by having a balled hydrophobic exterior in the complexed form and showing conformational flexibility.

The crystal structures of the uncomplexed form[4] and the potassium complexed form[5] of nonactin, which are given in Figures 1 and 2, respectively, demonstrate the conformational flexibility of the molecule. The uncomplexed form has roughly S_4 symmetry in the solid state, and from PMR studies it appears that this structure and others are present in solution.[1,6] The K^+, Na^+, Cs^+, and NH_4^+ complexed structures for nonactin have all been solved.[5] They all adopt a very similar conformation, which has the cation sitting at the center of a cube formed from four ether and four carbonyl oxygens for a coordination number of eight.[1] This arrangement is obtained by twisting the molecule into a conformation that has been described as a seam of a tennis ball.[1]

Figure 3 gives a schematic representation of nonactin. There are several important things to note: first, the molecule consists of a single "residue" that is repeated four times. However, two of these residues have configurations around the methyl groups of *SS* and two are *RS*. This leads to an alternating *RS*, *SS*, *RS*, and *SS* pattern which when folded together in the complex form places the *RS* and *SS* residue pairs opposite one another. This observation will be important when we consider reaction pathways for ion association.

(1) (a) Cram, D. J. *Science* **1988**, *240*, 760. (b) Rebek, J. R. *Science* **1987**, *235*, 1478. (c) Lehn, J.-M. *Angew. Chem., Int. Ed. Engl.* **1988**, *27*, 89.
(2) (a) Dobler, M. *Ionophores and Their Structures*; Wiley: New York, 1981. (b) Ovchinnikov, Y. A.; Yivanov, V.; Shkrob, A. M. *Membrane Active Complexones*; Elsevier: Amsterdam, 1974. (c) Eisenmann, G., Ed. *Membranes: A Series of Advances*; Marcel Dekker: New York, 1975; Vol. 3.
(3) (a) Kirch, M.; Lehn, J.-M. *Angew. Chem., Int. Ed. Engl.* **1975**, *14*, 555. (b) Deitrich, B. *J. Chem. Educ.* **1985**, *62*, 954.
(4) Dobler, M. *Helv. Chim. Acta* **1972**, *55*, 1371.
(5) (a) K^+ complex: Dobler, M.; Dunitz, J. D.; Kilburn, B. T. *Helv. Chim. Acta* **1969**, *52*, 2573. (b) Na^+ complex: Dobler, M.; Phizackerley, R. P. *Helv. Chim. Acta* **1974**, *57*, 664. (c) Cs^+ complex: Sakamati, T.; Iitaka, Y.; Nawata, Y. *Acta Crystallogr.* **1977**, *B33*, 52. (d) NH_4^+ complex: Neuport-Laves, K.; Dobler, M. *Helv. Chim. Acta* **1976**, *59*, 614.
(6) Prestegard, J. H.; Chan, S. L. *Biochemistry* **1969**, *8*, 3921.

0002-7863/92/1514-7542$03.00/0

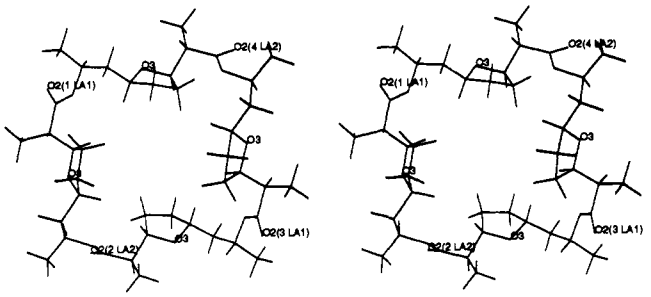

Figure 1. Stereoview of the crystal structure of uncomplexed nonactin.

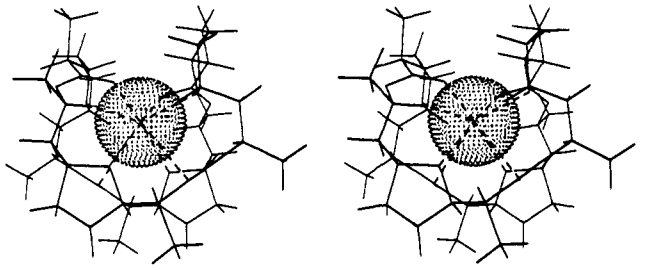

Figure 2. Stereoview of the crystal structure of nonactin complexed with potassium. All oxygen to ion distances are between 2.4 and 3.2 Å.

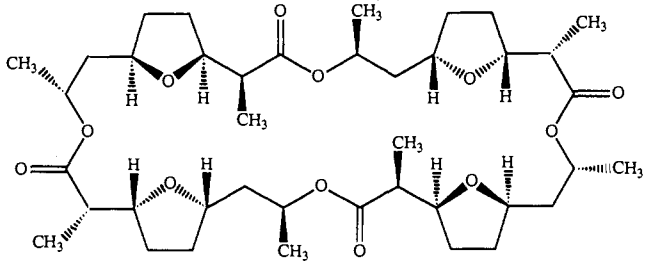

Figure 3. Schematic diagram of nonactin.

There are extensive data available in the literature for the free energy of binding of various cations to nonactin.[1,7] Because of the low solubility of nonactin in water, most of the binding data have been determined in methanol and ethanol. From these data and other studies the order of ion selectivity for nonactin is $NH_4^+ > K^+ > Rb^+ > Cs^+ > Na^+ > Ba^{2+}$.[1] Studies on nonactin in aqueous acetone have shown that as the mole fraction of water increases, the binding affinity for Na^+ decreases from −6.6 kcal/mol to −3.2 kcal/mol (for 39/61 water–acetone mole fraction).[8] Similar behavior is observed for other ions. Nonactin selectively binds K^+ over Na^+, with nonactin favoring the former by ~2.0 kcal/mol in MeOH.[7]

The pharmacological applications of naturally occurring ionophoric antibiotics (e.g., nonactin and valinomycin) depend on the ability to transport ions across a lipid bilayer. These molecules have been found to have fairly broad antimicrobial spectra and high activity against gram-positive bacteria, yeasts, and phytopathogenic fungi. However, the use of these compounds is limited in humans because of their high toxicity and the numerous physiological side effects these compounds produce. Some natural ionophores related to nonactin and valinomycin (e.g., nigericin[1]) have found use in the treatment of chicken coccidiosis,[9] and valinomycin has found application in rice farming, where it is used to keep phytopathogenic fungi under control.[10] Certain ionophores related to nonactin and valinomycin elicit a dramatic stimulation of the cardiovascular response in humans, which has led to the use of these compounds in the treatment of cardiac infarctions.[11]

Scheme I. Nonactin Thermodynamic Cycle for Calculation of $\Delta\Delta G_{bind}$

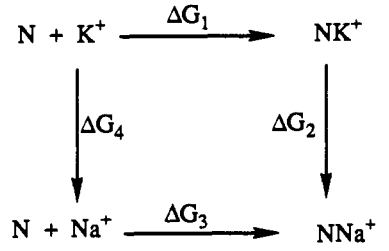

Other potential uses of ionophores include the distribution of radioisotopes in the body for use as a diagnostic tool or as a way to specifically target tumor cells in the treatment of cancer.[12]

Several theoretical efforts have provided insight into the molecular recognition properties of synthetic ionophores in aqueous and nonaqueous solvents.[13] Theoretical efforts have been reported for nonactin and were used to aid in the understanding of the conformational possibilities for nonactin and its cation selectivity.[14] However, these efforts were done in the gas phase, and gas-phase energy minimizations can only provide a static picture for this molecule.[14] Therefore, we have undertaken studies of nonactin in solvent with the goal of providing significant new insights into the function of this molecule.

Theoretical Background

Potential of mean force (PMF), molecular dynamics (MD), and free energy perturbation (FEP) simulations can provide molecular-level details regarding the binding of ions to nonactin and are used herein to provide insights into the molecular recognition process exhibited by nonactin.

FEP[15] simulations have been used to calculate the difference between the free energy of binding of potassium versus sodium to nonactin via the thermodynamic cycle shown in Scheme I. Given that free energy is a state function, the sum of the individual ΔG's of a cycle is zero. For the cycle given in Scheme I, eq 1 shows the free energy relationship. Rearrangement of eq 1 to solve for the relative free energy of binding, results in eq 2. In these

$$\Delta G_1 + \Delta G_2 - \Delta G_3 - \Delta G_4 = 0 \quad (1)$$

$$\Delta G_1 - \Delta G_3 = \Delta G_4 - \Delta G_2 = \Delta\Delta G_{bind} \quad (2)$$

simulations the potassium ion is slowly perturbed to sodium ion in solution (ΔG_4) and in the nonactin complex (ΔG_2). The values obtained in this way are then used to calculate the relative free energies of binding of the two ions. FEP simulations accumulate the free energy change as one state is slowly perturbed into another state.[15] In the "slow growth" method, which we have employed here, the perturbation occurs over a period of time via a coupling parameter, λ. A lambda value of 1 represents the initial state and a lambda value of 0 represents the final perturbed state. Lambda is slowly perturbed from 1 to 0 and the free energy change associated with the perturbation is determined from the equation:

(7) Izatt, R. M.; Bradshaw, J. S.; Nielson, S. A.; Lamb, J. D.; Christensen, J. J. *Chem. Rev.* **1985**, *85*, 271.
(8) Prestegard, J. H.; Chan, S. L. *J. Am. Chem. Soc.* **1970**, *92*, 4440.
(9) Shumard, R. F.; Callender, M. E. *Antimicrob. Agents Chemother.* **1967**, 369.
(10) Brown, R.; Brennan, J.; Kelley, C. *Antibiot. Chemother.* **1962**, *12*, 482.
(11) Pressman, B. C. *Fed. Proc.* **1973**, *32*, 1698.
(12) Semenoff, D.; Marzilli, L.; Strauss, H. W.; Harrison, K.; Rhodes, B. A.; Pitt, B. J. *Nucl. Med.* **1975**, *576*, 576.
(13) (a) Grootenhuis, P. D. J.; Kollman, P. A. *J. Am. Chem. Soc.* **1989**, *111*, 2152. (b) Lybrand, T. P.; McCammon, J. A.; Wipff, G. *Proc. Natl. Acad. Sci. U.S.A.* **1986**, *83*, 833. (c) Grootenhuis, P. D. J.; Kollman, P. A. *J. Am. Chem. Soc.* **1989**, *111*, 4046. (d) Mazor, M. A.; McCammon, J. A.; Lybrand, T. P. *J. Am. Chem. Soc.* **1989**, *111*, 56. (e) Mazor, M. A.; McCammon, J. A.; Lybrand, T. P. *J. Am. Chem. Soc.* **1990**, *112*, 4411. (f) Auffinger, P.; Wipff, G. *J. Am. Chem. Soc.* **1991**, *113*, 5976. (g) Auffinger, P.; Wipff, G. *J. Inclusion Phenom. Mol. Recognit. Chem.* **1991**, *11*, 71. (h) Auffinger, P.; Wipff, G. *J. Chim. Phys.* **1991**, *88*, 2525.
(14) See, for example: (a) Sakamaki, T.; Iitaka, Y.; Nawata, Y. *Acta Crystallogr.* **1976**, *B32*, 768. (b) Lee, Y. N.; Hamori, E. *Biopolymers* **1974**, *13*, 77. (c) Pullman, A. *Chem. Rev.* **1991**, *91*, 793. (d) Reference 5c.
(15) (a) Zwanzig, R. W. *J. Chem. Phys.* **1954**, *22*, 1420. For some recent reviews see: (b) van Gunsteren, W. F. *Protein Eng.* **1988**, *2*, 5. (c) Mezei, M.; Beveridge, D. L. *Ann. N.Y. Acad. Sci.* **1986**, *482*, 1. (d) Jorgensen, W. L. *Acc. Chem. Res.* **1989**, *22*, 184.

$$\Delta G = \sum_n [V(\lambda + \Delta\lambda) - V(\lambda)]_\lambda \quad (3)$$

V is the potential energy at a particular λ value. The change in potential energy is accumulated over every MD step, where n is the total number of steps to give the total change in free energy. It has become increasingly clear that FEP simulations are very sensitive to the relaxation time of the system under study.[16] Hence, it important to evaluate the convergence characteristics of our FEP simulations.

The PMF is determined using a free energy technique that determines the free energy change along a reaction coordinate.[17] In our work the PMF is accumulated as a function of the distance between the center of mass of the ion and of the ionophore.[17j] The ion is pulled out of the ionophore stepwise in a series of windows to obtain a free energy profile which can then be used to obtain an association constant. The association constant for the process is calculated via eq 4:

$$K_a = N\int_0^{r_c} 4\pi r^2 \exp[-W(r)/kT]\,dr \quad (4)$$

K_a is the association constant, $W(r)$ is the potential of mean force, k is Boltzmann's constant, T is temperature, N is Avogadro's number, and r_c is the cutoff distance for association. The association constant is then used to calculate the free energy of binding through eq 5 where ΔG is the absolute free energy of binding:

$$\Delta G = -RT \ln K_a \quad (5)$$

Not only does the PMF calculation provide energetic information about the binding process, it also provides structural information about the association process. MD trajectories run at points on the PMF profile yield structural information on the system along the reaction coordinate.

The MD and FEP simulations described in this paper were done in methanol, because binding data exist for nonactin in methanol,[1,7] and several theoretical models[18] exist that reproduce the properties of bulk methanol. To accurately model the complex we needed to develop parameters for the ionophores and the ions for the AMBER force field.[19] Much parametrization work and theoretical studies have been done for potassium and sodium in water;[20] however, little work has been done to describe these ions in nonaqueous solvents.[21] Usually, when these ions are studied in nonaqueous solvents standard water ion parameters sets are used. This is a reasonable approximation, but we have spent some time modifying and checking this procedure. Given these considerations the paper will be organized as follows. First, we will describe efforts aimed at deriving a set of parameters for nonactin followed by the determination of an accurate set of parameters for sodium and potassium in methanol. Next, we will present our FEP simulation results, and this will be followed by the PMF results for the association of potassium with nonactin.

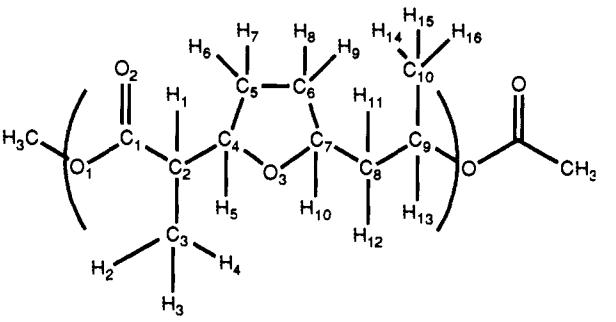

1

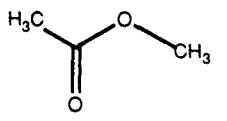

2

Figure 4. "Residues" used in the residue-based fitting procedure.

Table I. Nonactin Residue 6-31G* Charges

atom(s)	6-31G* charge	atom(s)	6-31G* charge	atom(s)	6-31G* charge
O1	−0.4395	O3	−0.3898	H10	0.0306
C1	0.8590	C5	−0.0690	C8	−0.4436
O2	−0.5655	H6	0.0259	H11	0.1595
C2	−0.2066	H7	0.0259	H12	0.1595
H1	0.1186	C6	0.0933	C9	0.1952
C3	−0.4510	H8	−0.0145	H13	0.0938
H2–H4	0.1434	H9	−0.0145	C10	−0.3493
C4	0.1941	C7	0.2242	H14–H16	0.1092
H5	0.0059				

Computational Procedure

Nonactin Parametrization. The first step was to develop the appropriate force field for the description of nonactin. We parametrized the all-atom AMBER[19] force field which has the form given in eq 6. The first three terms represent the "bonded"

$$E_{total} = \sum_{bonds} \frac{K_r}{2}(r - r_{eq})^2 + \sum_{angles} \frac{K_\theta}{2}(\theta - \theta_{eq})^2 + \sum_{dihedrals} \sum_n \frac{V_n}{2}[1 + \cos(n\phi - \gamma)] + \sum_{i<j} \epsilon_{ij}\left(\frac{R_{ij}^*}{R_{ij}}\right)^{12} - \left(\frac{R_{ij}^*}{R_{ij}}\right)^6 + \frac{1}{VDW_{scale}} \sum_{\substack{i<j \\ 1\text{-}4\ terms}} \epsilon_{ij}\left[\left(\frac{R_{ij}^*}{R_{ij}}\right)^{12} - \left(\frac{R_{ij}^*}{R_{ij}}\right)^6\right] + \sum_{H\text{-}bonds}\left[\frac{C_{ij}}{R_{ij}^{12}} - \frac{D_{ij}}{R_{ij}^{10}}\right] + \sum_{i<j} \frac{q_i q_j}{\epsilon R_{ij}} + \frac{1}{EE_{scale}} \sum_{\substack{i<j \\ 1,4\ terms}} \frac{q_i q_j}{\epsilon R_{ij}} \quad (6)$$

interactions present in a molecule, namely, the bond, angle, and torsion interactions. The bond and angle interactions are represented by a quadratic potential, while the torsional interactions are represented by a truncated Fourier series. K_X (where $X = r, \theta$) is the force constant for the bond or angle, while X_{eq} is the experimentally observed equilibrium bond length or angle associated with force constant K_X. X is the calculated value for the bond or angle. V_n, n, ϕ, and γ represent the torsional barrier, the periodicity, the calculated dihedral angle, and, finally, the phase. The next five terms represent the "nonbonded" interactions in a molecule. These are the Lennard-Jones (the $R_{ij}^{-12} - R_{ij}^{-6}$ or 6–12 terms), the hydrogen bond (the 10–12 terms), and the electrostatic interactions. R_{ij} is the distance between atoms i and j, R_{ij}^*, C_{ij}, and D_{ij} are parameters that define the shape of the Lennard-Jones

(16) Mitchell, M. J.; McCammon, J. A. *J. Comput. Chem.* **1991**, *2*, 271.
(17) (a) Prue, J. E. *J. Chem. Educ.* **1969**, *46*, 12. (b) Berkowitz, M.; Karim, O. A.; McCammon, J. A.; Rossky, P. J. *Chem. Phys. Lett.* **1984**, *105*, 577. (c) Dang, L. X.; Pettit, B. M. *J. Am. Chem. Soc.* **1987**, *109*, 5531. (d) Pettit, B. M.; Rosskyu, P. J. *J. Chem. Phys.* **1987**, *86*, 6560. (e) Ravishanker, G.; Mezei, M.; Beveridge, D. L. *Faraday Symp. Chem. Soc.* **1982**, *17*, 79. (f) Tobias, D. T.; Brooks, C. L., III *Chem. Phys. Lett.* **1987**, *142*, 472. (g) Patey, G. N.; Valleau, J. P. *J. Chem. Phys.* **1975**, *63*, 2334. (h) Pratt, L. R.; Chandler, D. *J. Chem. Phys.* **1977**, *67*, 3683. (i) Jorgensen, W. L.; Buckner, J. K.; Boudon, S.; Tirado-Rives, J. *J. Chem. Phys.* **1988**, *89*, 3742. (j) Dang, L. X.; Kollman, P. A. *J. Am. Chem. Soc.* **1990**, *112*, 5716. (k) Van Eerden, J.; Briels, W. J.; Harkema, S.; Feil, D. *Chem. Phys. Lett.* **1989**, *164*, 370. (l) Elber, R. *J. Chem. Phys.* **1990**, *93*, 4312.
(18) (a) Haughney, M.; Ferrerio, M.; McDonald, I. R. *J. Phys. Chem.* **1987**, *91*, 4934. (b) Jorgensen, W. L. *J. Phys. Chem.* **1986**, *90*, 1276. (c) Palinkas, G.; Hawlicka, E.; Heinzinger, K. *J. Phys. Chem.* **1987**, *91*, 4334.
(19) Weiner, S. J.; Kollman, P. A.; Nguyen, D. T.; Case, D. A. *J. Comput. Chem.* **1986**, *7*, 230.
(20) (a) Mezei, M.; Beveridge, D. L. *J. Chem. Phys.* **1981**, *74*, 6902. (b) Clementi, E.; Barsotti, R. *Chem. Phys. Lett.* **1978**, *59*, 21. (c) Chandrasekhar, J.; Spellmeyer, D. C.; Jorgensen, W. L. *J. Am. Chem. Soc.* **1984**, *106*, 903. (d) Impey, R. W.; Madden, P. A.; McDonald, I. R. *J. Phys. Chem.* **1983**, *87*, 5071. (e) Cieplak, P.; Kollman, P. A. *J. Chem. Phys.* **1990**, *92*, 6761. (f) Aqvist, J. *J. Phys. Chem.* **1990**, *94*, 8021.
(21) (a) Chandrasekhar, J.; Jorgensen, W. L. *J. Chem. Phys.* **1982**, *77*, 5080. (b) Rao, B. G.; Singh, U. C. *J. Am. Chem. Soc.* **1990**, *112*, 3803.

potential for the interaction between atoms i and j, q_i and q_j are th atomic point charges for atoms i and j, and ϵ is the dielectric constant.

The first set of parameters derived were the atomic point charges for the "residue" present in nonactin. This was accomplished using 6-31G* ab initio[22] electrostatic potential (ESP) calculations[23] in Gaussian 88.[24] The choice of 6-31G* is due to the fact that this basis set reproduces the electrostatic properties of molecules reasonably well.[22] For nonactin we evaluated ESP charges for **1** (Figure 4) which is the repeating unit in nonactin. In order to extract the ESP point charges for this residue, we constrained the ESP charges for the atoms out of the parentheses at the values obtained for **2**. In this way the charge neutrality of the complex was maintained as well as the reality of our model for obtaining point charges (i.e., the "residue" feels its nearest bonded neighbors). Once the fitting was done, we averaged hydrogens on methyl groups. The charges for the residue can be found in Table I.

For the present work, bond, angle, torsion, and Lennard-Jones 6–12 parameters were taken directly from AMBER.[19] The starting geometry was the crystal structure for the potassium complex of nonactin.[5]

Ion Parametrization. We parametrized the potassium and sodium ions to reproduce the absolute free energies of solvation of the ions in methanol and the expected coordination numbers for the first solvation shell. The Lennard-Jones parameters were adjusted while the charges on the ions remained +1. The absolute free energies were calculated by perturbing the ion into a dummy atom with no charge or Lennard-Jones interactions. For the FEP simulation details, see the description of the simulation protocol given below. We applied the Born correction[25] to account for the long-range electrostatic interactions. The correction is −16.1 kcal/mol for a monovalent ion in methanol when the nonbonded cutoff is 10 Å. This correction is qualitative in nature and has been extensively studied elsewhere.[25] This procedure is a simple but powerful tool to account for long-range electrostatic interactions.[25]

The final Lennard-Jones parameters are R^* = 2.17 Å and ϵ = 0.035 kcal/mol for K^+ and R^* = 1.70 Å and ϵ = 0.04 kcal/mol for Na^+. The absolute free energies for the ions can be found along with the coordination numbers in Table II. The values for ΔG_{solv} in Table II are the free energies of solvation calculated from the perturbation of the ion to a dummy atom with no charge or Lennard-Jones interactions. The values for ΔG_{corr} in Table II are the calculated free energies corrected by the addition of the Born correction. Figure 5 contains the radial distribution function (rdf) for each ion in methanol. The coordination numbers were calculated by integrating the first peak of the rdf. The coordination numbers are equal to those of the ions in water,[26] and the first peak of the rdf occurs at a slightly higher value than water.[26] This result can be explained by the fact that methanol is bulkier than water which results in steric hindrance that does not allow the methanol oxygens to get as close to the ions. Regardless, the calculated rdf and coordination are similar to that observed for water, which is not unreasonable.[21a] The calculated free energy of solvation for both potassium and sodium are ~10 kcal/mol too large when compared with experiment. Using this parameterization method, it is possible to obtain quantitative agreement with experiment for this quantity, but the coordination environment and rdf first peak position are very poorly reproduced. Hence, we decided to get the best set of compromise parameters

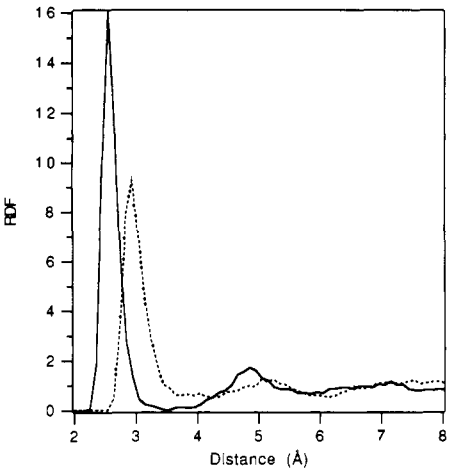

Figure 5. Radial distribution function of K^+ (dashed line) and Na^+ (solid line) in methanol.

Table II. Results of Ion Parameterization

	K^+	Na^+
ΔG_{solv} (kcal/mol)	−64.3 ± 0.9	−84.8 ± 0.8
ΔG_{corr} (kcal/mol)	−80.4 ± 0.9	−100.9 ± 0.8
ΔG_{exp} (kcal/mol)[a]	−70.3	−87.6
peak position (Å)	2.95	2.56
coord. no.	6	6
H_2O peak position[b]	2.7	2.35
H_2O coord no.[b]	6	6

[a] See ref 30. [b] See ref 26.

that reasonably reproduced both the free energy of solvation and structural environment of these ions. In our opinion this set of parameters is probably the best we can do within the effective two-body model. Further improvement will require consideration of polarization effects.[27]

Simulation Protocols

The FEP simulations and the MD trajectories for the ions in methanol were done at constant pressure (1 atm) and constant temperature (298 K). SHAKE was employed to restrain the bond lengths to their equilibrium distances in order to remove the high frequency motions.[28] This allowed us to use a timestep of 1.5 fs. The nonbond cutoff for interactions was 10 Å and the nonbond pair list was updated every 25 MD steps. The FEP simulations for K^+ to Na^+ in both the complexed state and the free ion were initially done over a period of 45 ps. All ion parametrization work was done using 45-ps timescales. Jorgensen's methanol model was used as the solvent model.[18b] All simulations were done with the AMBER[31] suite of programs.

The PMF and MD simulations at the critical points along the reaction path were done at constant volume and constant temperature (300 K). The SHAKE[28] algorithm and a 1.5-fs timestep were used. The ion and the ionophore were solvated by a total of 646 methanol molecules in a box 38.3 Å × 38.3 Å × 36.0 Å. The starting structure was the potassium complex crystal structure minimized in the methanol box. The distance from the center of mass of nonactin to the center of mass of potassium was incremented by ±0.25 Å to a distance 9 Å from the starting structure, except from 0.0 to 1.0 Å, 2.5 to 5.0 Å, and 6.0 to 9.0 Å where the increment was ±0.125 Å. These regions were sampled more thoroughly because they were statistically noisy using the coarser mesh, and we wanted to obtain more precise information on the chemical changes occurring at these positions. A total of 27 ps of MD was done at each coordinate separation with 9 ps used for equilibration and 18 ps used for sampling. The nonbond cutoff was 9 Å, and the nonbond pair list was updated every 10 steps. A total of 32 individual simulations (864 ps total) were carried out to assemble the entire PMF profile.

(22) Hehre, W. J.; Radom, L.; Schleyer, P. v. R.; Pople, J. A. *Ab Initio Molecular Orbital Theory*; John Wiley: New York, 1986.
(23) (a) Williams, D. E.; Yan, J.-M. *Adv. At. Mol. Phys.* **1988**, *23*, 87. (b) Chirlian, L. E.; Francl, M. M. *J. Comput. Chem.* **1987**, *8*, 894. (c) Singh, U. C.; Kollman, P. A. *J. Comput. Chem.* **1984**, *5*, 129.
(24) GAUSSIAN 88: Frisch, M. J.; Head-Gordon, M.; Schlegel, H. B.; Raghavachari, K.; Binkley, J. S.; Gonzalez, C.; Defrees, D. J.; Fox, D. J.; Whiteside, R. A.; Seeger, R.; Melius, C. F.; Baker, J.; Martin, R.; Kahn, L. R.; Stewart, J. J. P.; Fluder, E. M.; Topiol, S.; Pople, J. A. Guassian Inc.: Pittsburgh, PA, 1988.
(25) Straatsma, T. P.; Berendsen, H. J. C. *J. Chem. Phys.* **1988**, *89*, 5876.
(26) Marcus, Y. *Chem. Rev.* **1988**, *88*, 1475.
(27) Dang, L. X.; Rice, J. E.; Caldwell, J. A.; Kollman, P. A. *J. Am. Chem. Soc.* **1991**, *113*, 2481 and references cited therein.
(28) Ryckert, J. P.; Ciccotti, G.; Berendsen, H. J. C. *J. Comput. Phys.* **1977**, *23*, 327.
(29) Straatsma, T. P.; McCammon, J. A. *J. Chem. Phys.* **1989**, *91*, 3631.
(30) Marcus, Y. *Ion Solvation*; John Wiley: New York, 1985.
(31) AMBER 3.0: Singh, U. C.; Weiner, P. K.; Caldwell, J.; Kollman, P. A.

Table III. Free Energy Convergence for $K^+ \rightarrow Na^+$

time for perturbation (ps)	free energy (kcal/mol)
45	−17.4 ± 0.3
90	−17.7 ± 0.1
180	−17.5 ± 0.1

Table IV. Results of Free Energy Perturbation for Nonactin

perturbation	ΔG (kcal/mol)
$K^+ \rightarrow Na^+$	−17.4 ± 0.3
$NK^+ \rightarrow NNa^+$	−16.4 ± 0.7
$\Delta\Delta G_{bind}$	−1.0 ± 0.8
$\Delta\Delta G_{bind}$ (exp)[a]	−2.0 ± 0.7

[a] Averaged from values given in ref 7.

Results and Discussion

Relative Binding Free Energy. Table III contains the results of the convergence tests for the perturbations of potassium to sodium in solution. The starting configuration was equilibrated for 27 ps. The perturbation was done over 45, 90, and 180 ps in both the forward and the reverse directions. The values obtained at 45 ps are within the error bars of the longer simulations. Thus, the perturbation run appears converged at 45 ps. The FEP value for this system was calculated by averaging the forward and reverse perturbations for three temporally (18 ps) separated runs using the 45-ps timescale. The same type of convergence test was applied to the ion in nonactin. The starting structure was equilibrated for 27 ps at the first minimum shown in the PMF profile (see Figure 6), and the center of mass of the ion and the nonactin molecule were held fixed relative to one another. Perburation runs were done from this starting structure at 45-, 90-, and 180-ps timescales. The ion drifted out of the complex during perturbation runs greater than 45 ps and prevented sampling of the ion perturbed in the complex. Hence we were forced to use the shorter timescale of 45 ps for all of our runs. Three temporally (18 ps) separated runs were averaged to give the value in Table IV. The calculated (−1.0 ± 0.8 kcal/mol) difference in the free energy of binding for K^+ and Na^+ fall within the range of experimental values for the system in methanol (−2.0 ± 0.7 kcal/mol).[7] Reproduction of the experimental relative binding affinities gave us confidence in our model, but a much more stringent test would be to evaluate the absolute free energy of binding for one of the ions.

PMF Results. The PMF profile can be found in Figure 6. The PMF path proceeded along the $+z$ direction in our simulation, and no variations of the x and y coordinates of the ion and nonactin centers of mass were allowed. However, nonactin was capable of rotating along the x, y, and z axes as long as the center of mass position was maintained. Examination of nonactin showed that there are only two reasonable pathways, which are $+z$ or $-z$ in the orientation of the crystal structure Cartesian coordinates. One pulls the ion through the *SS* residues and the other through the *RS* ones. Graphical examination of these pathways indicated that they are essentially identical except in chirality. Thus, we only examined the PMF along one of these two pathways.

Analysis of the PMF profile reveals two minima at 1.0 Å and 4.0 Å from the initial crystal structure and a maximum at 2.75 Å from the initial crystal structure. The shift of the minimum to 1 Å from the crystal structure is not surprising, because the ion could come into contact with solvent on one side in an energetically favorable arrangement while being ligated by nonactin on the other side. Dang and Kollman have seen a similar shift for the minimum in 18-crown-6 in water.[17j]

Structures from the PMF profile with a separation of 1.0 to 9.0 Å in 1.0-Å increments can be found in Figure 7. The structures are the final coordinates from the PMF simulations at the respective separation distances and are representative of the nonactin potassium complex at these distances. Inspection of the structures gives an overall representation of the association process of nonactin with potassium along a linear pathway. The ion approaches nonactin, and nonactin responds by coordinating the ion with two

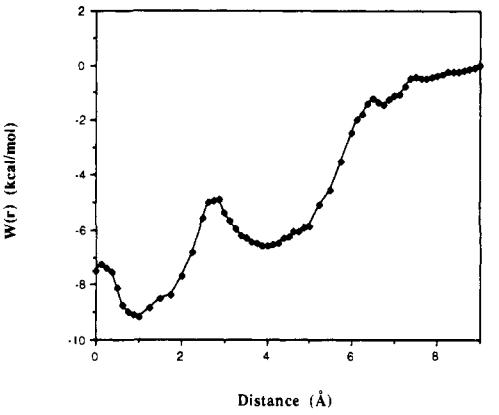

Figure 6. PMF profile for the association of nonactin and K^+ in methanol.

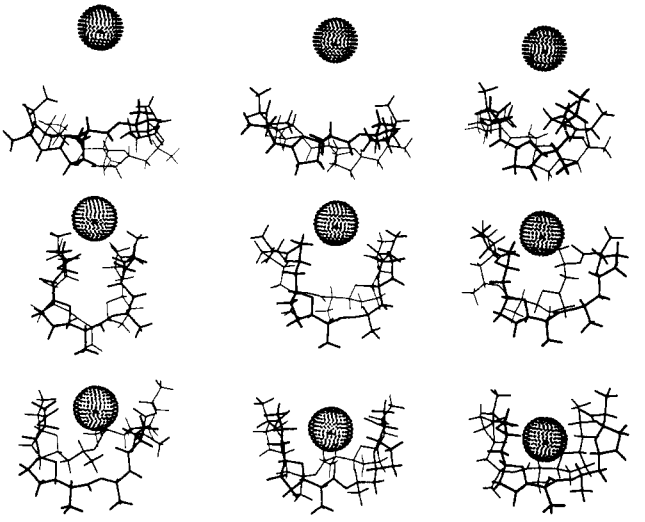

Figure 7. Representative structures along the PMF profile. The separation distances are 9, 8, 7, 6, 5, 4, 3, 2, and 1 Å, respectively, viewing the figure from top to bottom/left to right.

carbonyl oxygens (~6 Å). These carbonyls displace two methanol molecules in the first coordination shell. Nonactin then coordinates the ion with several of the remaining ether and carbonyl oxygens (~1.0 Å) which displaces several methanol molecules from the first coordination shell.

Analysis of molecular dynamics trajectories at the minima and the "transition state" provide more detail than the static structures in Figure 7. Analysis of the endpoint of the PMF profile (free nonactin) provides no information about the ion binding process. Conformational flexibility of free nonactin in methanol could be addressed through MD trajectories as others have done for uncomplexed 18-crown-6 in water;[29] however, this is beyond the scope of the work done here. Each inflection point was equilibrated for 63 ps and sampled for 72 ps with coordinates saved every 75 fs. We plotted the histograms of the ring, carbonyl, and methanol oxygen to K^+ distances to obtain coordination details of the ion at the inflection points. Figure 8a shows the carbonyl oxygen to K^+ distance histogram for a center of mass separation of 1.0 Å. We consider any atom less than 4.0 Å from the potassium to be coordinated. We chose this reference distance because the first peak of the K^+ to methanol oxygen rdf terminates at approximately 4.0 Å for our potassium model. On average, all four carbonyl oxygens are between 2.5 and 4.0 Å from the ion at the 1-Å separation and are therefore considered to be coordinated to the potassium ion. At a distance of 2.75 Å, the carbonyls shift away from the ion as shown in Figure 8b. The histogram of carbonyls at 4.0 Å (Figure 8c) shows three distinct peaks. The areas of these peaks give a ratio of 2:1:1. On average, two carbonyls are within the 2–4.0-Å region, while one is between 4 and

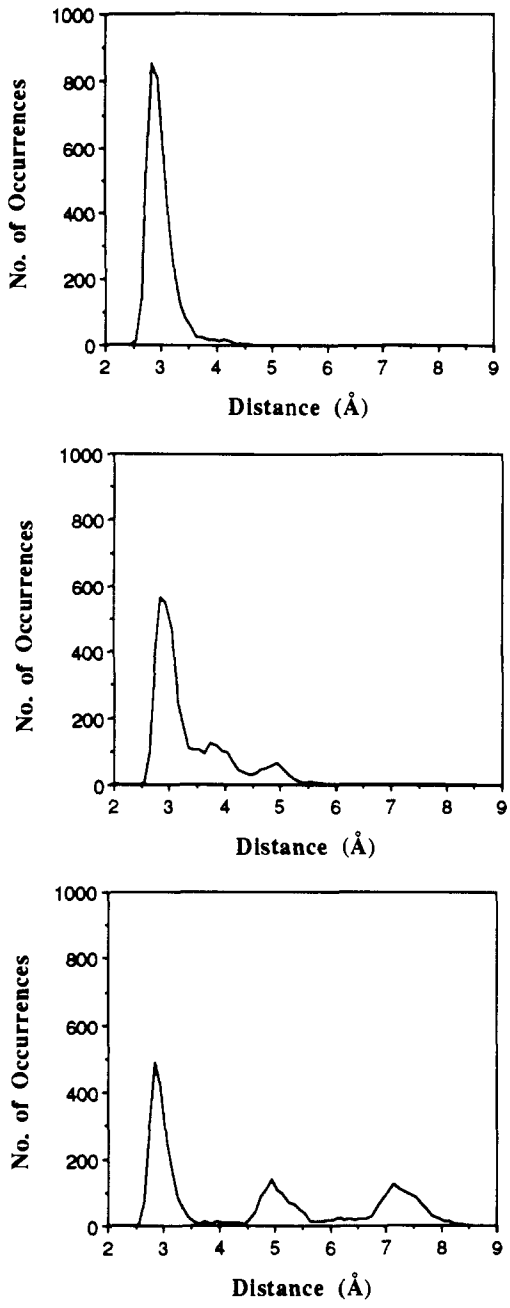

Figure 8. (a) K^+ to carbonyl oxygen distance histogram at 1.0-Å separation. (b) K^+ to carbonyl oxygen distance histogram at 2.75-Å separation. (c) K^+ to carbonyl oxygen distance histogram at 4.0-Å separation.

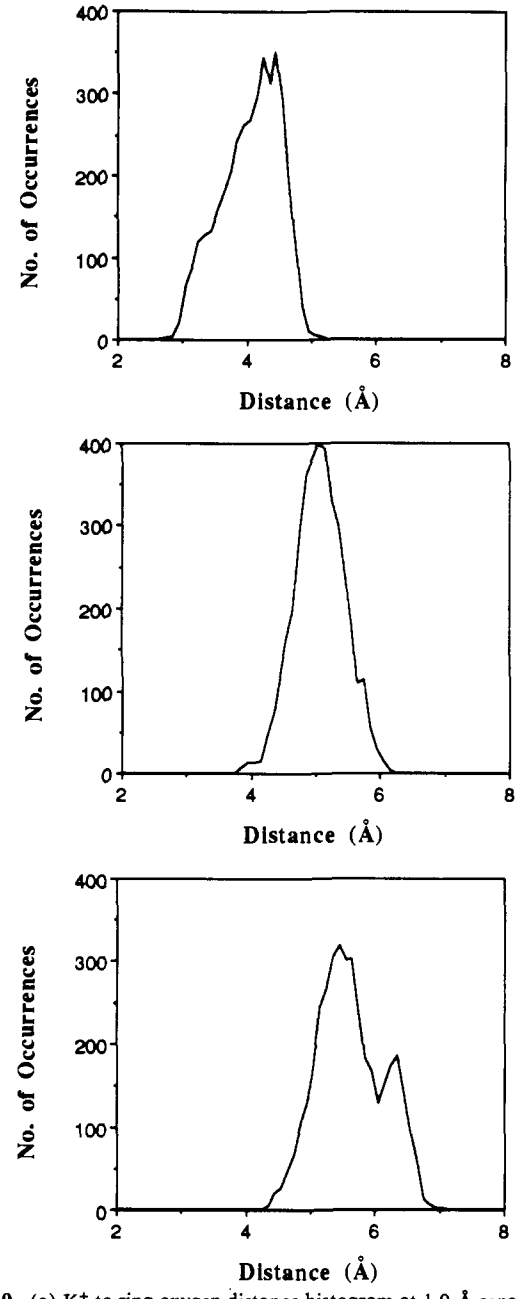

Figure 9. (a) K^+ to ring oxygen distance histogram at 1.0-Å separation. (b) K^+ to ring oxygen distance histogram at 2.75-Å separation. (c) K^+ to ring oxygen distance histogram at 4.0-Å separation.

6 Å and the remaining one is between 6 and 8 Å. Hence, the first two are still coordinating the ion while the last two are not directly coordinating to the ion. Figure 9 contains the histogram of the ring oxygens analyzed over the same coordinate sets. At the 1-Å separation, integration of Figure 9a from 0 to 4 Å indicates that out of a possible four ring oxygens only two are coordinated to the ion. At a separation of 2.75 Å, the ring oxygens ligate the K^+ only a small fraction of the time as seen in Figure 9b. The average coordination at this point is 0.4. Figure 9c shows no ring oxygen coordination at the 4.0-Å separation.

We also have averaged the number of methanol oxygens found within 4.0 Å of the K^+ at these three points to obtain information on how many methanol oxygens surround the ion. These results were calculated over 72 ps using the same coordinates sets used for the other oxygen histograms. We summarize these results along with the other histogram results in Table V. At a separation of 1 Å we find that there are four carbonyl oxygens, two ring oxygens, and two methanol oxygens coordinating the potassium

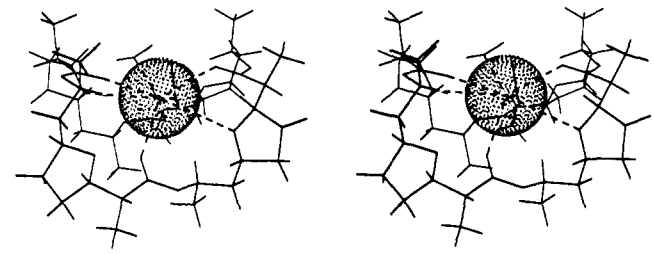

Figure 10. Stereoview of a representative structure at 1.0-Å separation. All oxygen to ion distances (dashed lines) are between 2.8 and 3.7 Å.

ion. This results in a net coordination of eight, which is the coordination number seen in the X-ray structure for the complexed form of this ionophore. At 2.75 Å we find three and one-half carbonyl oxygens, almost one-half of a ring oxygen, and about three methanol oxygens. The ion at this point has on average approximately seven nearest neighbors. Hence, the difference in coordination at the 1.0-Å to 2.75-Å separations is one. The

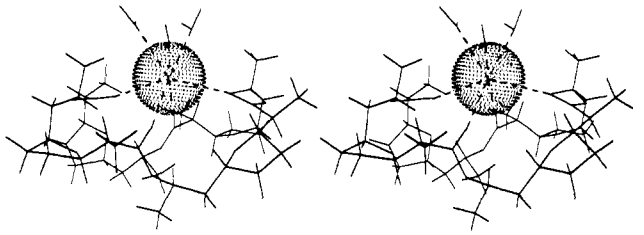

Figure 11. Stereoview of a representative structure at 2.75-Å separation. All oxygen to ion distances (dashed lines) are between 2.8 and 3.5 Å.

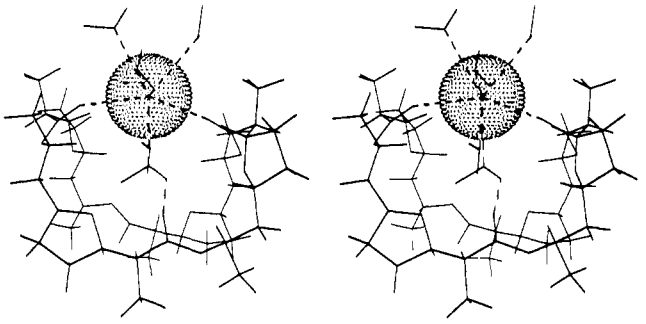

Figure 12. Stereoview of a representative structure at 4.0-Å separation. All oxygen to ion distances (dashed lines) are between 2.8 and 3.4 Å.

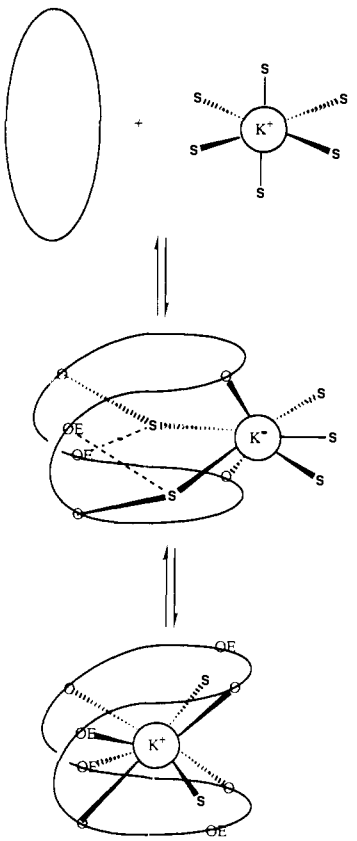

Figure 13. Schematic diagram of association of nonactin and K^+ in methanol.

minimum at 4.0 Å has two carbonyl oxygens, zero ring oxygens, and about five methanol oxygens for a total of seven nearest neighbors. Given that the coordination number is roughly the same at both the 2.75-Å and 4.0-Å points, it is interesting to attempt to understand why the 4.0 point is so stable relative to the 2.75-Å point. This is best done by comparison of the structure of the nonactin/ion complexes along the reaction path.

Figures 10, 11, and 12 show representative structures of the MD trajectories at the 1.0-Å, 2.75-Å, and 4.0-Å separations, respectively. These structures pictorially represent the analysis

Table V. Ion Coordination at Inflection Points of PMF Profile

	oxygen coordination		
separation, Å	carbonyl	ring	MeOH
1.0	4.0	2.0	1.9
2.75	3.5	0.4	2.9
4.0	2.0	0	4.9

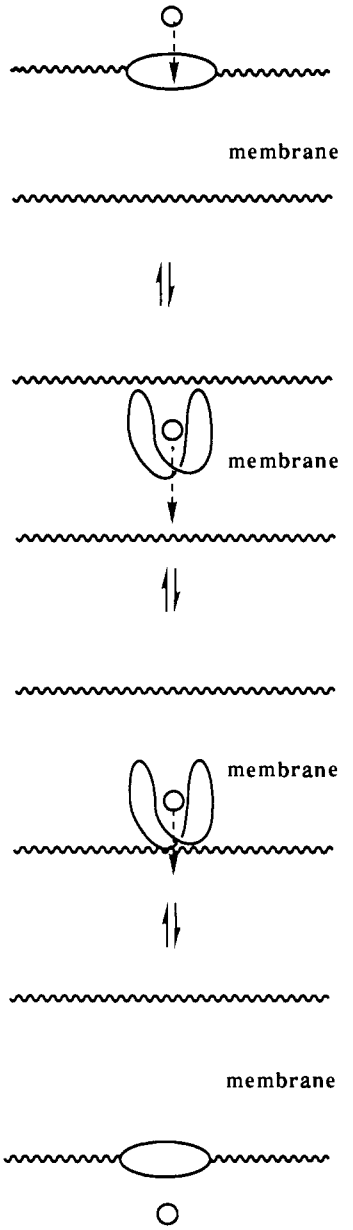

Figure 14. Schematic diagram of a possible nonactin transport pathway.

summarized in Table V. At the 4.0-Å separation distance, two interior methanols can form hydrogen bonds with nonactin carbonyls or ring oxygens while ligating the ion to stabilize the complex at this separation. They are also capable of hydrogen bonding to each other. These methanols dynamically form hydrogen bonds in several configurations with no one configuration dominating. Comparing the structure at the 2.75-Å separation distance to the 4.0-Å separation distance, the two methanols that were forming the hydrogen bonds are stripped from the ion. Although the coordination number at these two points are the same, the loss of the ability to hydrogen bond to the coordinated interior methanols contributes to the destabilization of the structure at the 2.75-Å separation with respect to the structure at the 4.0-Å separation.

From the PMF profile we can estimate an association constant for the complexation of nonactin with an ion. The choice of r_c

is very important in order to obtain realistic results. The usual choice is at the solvent separated point along the PMF profile. This can be somewhat subjective, but careful graphical analysis can identify this point. The ion is found to be solvent-separated at a 6.5-Å separation distance. Integrating from the 0-Å separation distance as the reference to 6.5 Å yields a K_a value of 49 700 (or −6.4 kcal/mol). Our calculated free energy of association is slightly higher than the experimental value of −5.5 ± 0.6 kcal/mol, but compares with experiment quite well. The calculated value represents only the value obtained by binding in the z direction. Binding in the $-z$ direction should be similar, but alternate routes could provide differing binding constants. These other routes may involve slight changes in the x or y directions, but given the stabilizing structural features observed along the reaction path (e.g., buttressing of methanols between nonactin and the ion), which would be destabilized owing to motions in these directions, we are reasonably confident that the path we have studied is a low-energy pathway. Furthermore, the excellent agreement between the experimental and theoretical binding constants gives us confidence that our pathway and the structural features along it give a reasonable representation of nonactin/potassium complexation process.

Conclusions

We find that by using an effective two-body potential we are able to accurately represent the association of an ion with the antibiotic ionophore nonactin. Further improvements could be made especially in the treatment of polarization effects[27] which would allow for an improved representation of the solvation of potassium and sodium in methanol. Regardless, we have been able to reasonably reproduce the relative binding affinities of nonactin for potassium and sodium (−1.0 ± 0.8 kcal/mol (calc) versus −2.0 ± 0.7 kcal/mol (expt)[7]), and, furthermore, we have been able to accurately reproduce the absolute free energy of binding of potassium to nonactin (−6.4 kcal/mol (calc) versus −5.5 ± 0.6 kcal/mol (expt)[7]).

We present a schematic of the association process of nonactin with potassium in Figure 13. Initially nonactin displaces two methanol molecules and replaces them with carbonyls (O). This gives the first minimum at 4.0 Å, which has five methanols and two nonactin carbonyls associated with the ion. Passing through the transition state at 2.75 Å gives the most stable point on this profile at a 1-Å separation distance. To reach this point three methanols are displaced and are replaced by two carbonyl oxygens (O) and two ether oxygens (OE). Thus, at this point we have a net coordination of eight.

The remarkable feature of this PMF is the role that the carbonyl oxygens play in the recognition process. Initially the ion is six-coordinated (first solvation shell) in methanol and nonactin recognizes the first coordination shell of the ion by making two hydrogen-bonding contacts at around 6.5-Å separation (nonactin carbonyl to methanol hydrogen). Two of the methanols in this shell are then displaced and replaced by two carbonyls from nonactin, while the other two carbonyls dynamically form and break hydrogen bonds with the two interior methanols. The final displacement brings into play two of the ether oxygens, which overall play a limited role.

Given our results it is interesting to speculate on how nonactin might function in a biomembrane. Nonactin is likely to rest on the membrane surface, and once it recognizes an ion it becomes balled up, which makes it hydrophobic. The ionophore then penetrates into the bilayer and makes its way to the other side. Interestingly, nonactin has two equivalent faces that allows the molecule to traverse the bilayer without rotating to expose the face into which the ion had originally entered. To complete the whole transport function, nonactin must finally ball up again without an ion and makes its way across the membrane to the starting face. This pathway is schematically given in Figure 14. Similar schemes have been proposed for other ionophores.[1]

Acknowledgment. Helpful discussions with Liem Dang and Olaf Andersen are greatly appreciated. This research was supported by the ONR (N00014-90-3-4002) and ACS-PRF (23225-G6,4) and their support is acknowledged. We also thank the Pittsburgh Supercomputer Center for CRAY YMP time and the Center for Academic Computing for IBM 3090 time.

Registry No. K^+, 7440-09-7; Na^+, 7440-23-5; nonactin, 6833-84-7.

Supplementary Material Available: Listing of important dihedral angles in nonactin which were analyzed statically at each point on the PMF profile (6 pages). Ordering information is given on any current masthead page.

Ab Initio Calculations on *m*-Quinone. The Ground State Is a Triplet

Raymond C. Fort, Jr.,[1a] Stephen J. Getty,[1b] David A. Hrovat,[1b] Paul M. Lahti,[1c] and Weston Thatcher Borden*,[1b]

Contribution from the Departments of Chemistry, University of Washington, Seattle, Washington 98195, and University of Massachusetts, Amherst, Massachusetts 01003.
Received March 27, 1992

Abstract: The geometries of the $^3B_2$, $^1B_2$, and $^1A_1$ states of *m*-quinone (**2**) have been optimized, using the 6-31G* basis set at, respectively, the UHF, ROHF, and GVB levels. Partial geometry reoptimization was carried out at the π-SDCI level. Calculations that included σ,π correlation also were performed. The triplet is predicted to be the ground state by 10.4 kcal/mol at the π-SDCI level and by 7.6 kcal/mol at the σ-S, π-SDCI level of theory. A value of 9.5 kcal/mol is calculated for the singlet-triplet splitting in *m*-quinodimethane (**1**) at the π-SDCI level. The apparent lack of effect on the singlet-triplet splitting of replacing the CH_2 groups in **1** by the oxygens in **2** is discussed.

In agreement with experiment[2] and with qualitative theoretical expectations,[3] previous calculations[4,5] on *m*-quinodimethane[6] (**1**) have found this diradical to have a triplet ground state. Previous calculations also have revealed that the replacement of the CH_2

(1) (a) On leave at the University of Washington from the Department of Chemistry, University of Maine, Orono, ME 04469. (b) University of Washington. (c) University of Massachusetts.

(2) Wright, B. B; Platz, M. *J. Am. Chem. Soc.* **1983**, *105*, 628.

(3) Borden, W. T.; Davidson, E. R. *J. Am. Chem. Soc.* **1977**, *99*, 4587. Review: Borden, W. T. In *Diradicals*; Borden, W. T., Ed.; Wiley: New York, 1982; pp 1-72.

0002-7863/92/1514-7549$03.00/0